



## Structural resemblances and comparisons of the relative pharmacological properties of imatinib and nilotinib

Paul W. Manley<sup>a,\*</sup>, Nikolaus Stiefl<sup>a</sup>, Sandra W. Cowan-Jacob<sup>a</sup>, Susan Kaufman<sup>a</sup>, Jürgen Mestan<sup>a</sup>, Markus Wartmann<sup>a</sup>, Marion Wiesmann<sup>a</sup>, Richard Woodman<sup>b</sup>, Neil Gallagher<sup>c</sup>

<sup>a</sup> Novartis Institutes for BioMedical Research, Basel, Switzerland

<sup>b</sup> Novartis Pharmaceuticals Corporation, East Hanover, New Jersey, USA

<sup>c</sup> Novartis Pharmaceuticals AG, Basel, Switzerland

### ARTICLE INFO

#### Article history:

Received 9 March 2010

Revised 8 July 2010

Accepted 11 August 2010

Available online 14 August 2010

#### Keywords:

Imatinib

Nilotinib

BCR-ABL1

CSF-1R

CML

Similarity

Adverse events

Tanimoto

### ABSTRACT

Although orphan drug applications required by the EMEA must include assessments of similarity to pre-existing products, these can be difficult to quantify. Here we illustrate a paradigm in comparing nilotinib to the prototype kinase inhibitor imatinib, and equate the degree of structural similarity to differences in properties. Nilotinib was discovered following re-engineering of imatinib, employing structural biology and medicinal chemistry strategies to optimise cellular potency and selectivity towards BCR-ABL1. Through evolving only to conserve these properties, this resulted in significant structural differences between nilotinib and imatinib, quantified by a Daylight-fingerprint–Tanimoto similarity coefficient of 0.6, with the meaning of this absolute measure being supported by an analysis of similarity distributions of similar drug-like molecules. This dissimilarity is reflected in the drugs having substantially different preclinical pharmacology and a lack of cross-intolerance in CML patients, which translates into nilotinib being an efficacious treatment for CML, with a favourable side-effect profile.

© 2010 Elsevier Ltd. All rights reserved.

### 1. Introduction

The notion of similarity appertains to relative comparisons and, in the absence of recognised paradigms for quantitative assessment of drug similarity, these are frequently qualitative and involve subjective preconceptions. Despite the difficulties, comparisons between molecules to provide quantitative assessments of ‘similarity’ are becoming increasingly important for the prediction of molecular properties, as well as for procedures such as Health Authority registration.<sup>1,2</sup> As an example of the latter, the European Medicines Agency (EMA) may designate a medicinal product as an orphan drug through applying the ‘prevalence’ criterion, whereby the sponsor should establish that it is intended for the diagnosis, prevention or treatment of a life-threatening or chronically debilitating condition affecting no more than 5 in 10 thousand persons.<sup>3,4</sup> Orphan drug designation can lead to several

incentives, including expedited Health Authority review and a period of market exclusivity upon authorisation. As part of an orphan drug application, where two products are potentially similar, the applicant of the second product is required to provide appropriate documentation on its position regarding similarity with reference to mechanism of actions and structural similarity. The criteria to assess similarity are recommended in the European Commission guideline on aspects of the application of Article 8(1) and (3) of Regulation (EC) No. 141/2000.<sup>4</sup> Thus Section 2, Article 3 of Commission Regulation (EC) No 847/2000 defines a similar active substance as ‘an identical active substance or an active substance with the same principal molecular structural features (but not necessarily all of the same molecular structural features) and which acts via the same mechanism’. The guidelines go on to say that since molecules exert their biological action in solution, differences seen by X-ray crystallography in the crystalline state may not be relevant for the assessment of similarity. It is also suggested that computational methods may be used to measure the degree of structural similarity between molecules, many of which allow ‘similarity searching’ to identify molecules having common or similar molecular architectural features (two- or three-dimensional).

Consequently, in this study of drug similarity, two tyrosine kinase inhibitors, possessing activity against BCR-ABL1 and

Abbreviations: BCR-ABL1, breakpoint cluster region-Abelson fusion protein; CML, chronic myeloid leukaemia; DDR, discoidin domain receptor; PDGFR, platelet-derived growth factor receptor; KIT, stem cell factor receptor; CSF-1R, colony stimulating factor-1 receptor.

\* Corresponding author. Address: Novartis Pharma AG, WKL-136.4.86, Klybeckstrasse 141, CH-4002 Basel, Switzerland. Tel.: +41 616966878; fax: +41 616962455.

E-mail address: [paul.manley@novartis.com](mailto:paul.manley@novartis.com) (P.W. Manley).

developed for the treatment of chronic myelogenous leukaemia (CML), are compared on the basis of structural similarity, target selectivity and general biological activity in patients. CML is caused by unfaithful repair of a double-strand DNA break in a pluripotent haematopoietic cell, which results in the formation of the Philadelphia chromosome (Ph), t(9,22), that carries the breakpoint cluster region-Abelson fusion gene, *BCR-ABL1*.<sup>5</sup> This oncogene encodes the chimeric BCR-ABL1 protein, having a constitutively activated ABL1 tyrosine kinase domain that deregulates intracellular signalling pathways and causes CML. Following the discovery of imatinib (Gleevec®; Fig. 1a) as an inhibitor of the BCR-ABL1 kinase,<sup>6,7</sup> this effective, safe and well-tolerated drug has become the standard of care for the treatment of newly diagnosed Ph+ CML patients in chronic phase and set a new paradigm for the treatment of cancer with molecularly target drugs.<sup>8</sup> However, whereas about 85% of newly diagnosed chronic phase (CP) patients achieve a complete cytogenetic response to imatinib, patients harbour minimal residual disease that can eventually lead to relapse. Relapse, which is a more common occurrence in the advanced, accelerated phase (AP) and blast phase (BC) stages of the disease, is most frequently due to the emergence of clones expressing mutant forms of the BCR-ABL1 protein kinase in which single amino-acid substitutions lead to a reduced sensitivity towards imatinib.<sup>9</sup>

Nilotinib (Tasigna®; Fig. 1b) is a novel tyrosine kinase inhibitor which has been developed to address the unmet medical need associated with imatinib-intolerance and imatinib-resistance in chronic and advanced phases of CML.<sup>10,11</sup> As such nilotinib is a highly potent and selective inhibitor of the *wild-type* BCR-ABL1, which maintains activity against the majority of imatinib-resistant mutants, and has few off-target activities.<sup>11–13</sup> This preclinical profile supports nilotinib as an effective treatment of chronic and advanced Ph+ CML patients, whose disease cannot be controlled by imatinib.<sup>14,15</sup>

Nilotinib emerged from a rational, structure-based drug discovery programme, in which the imatinib structure was reengineered,<sup>11,16</sup> to incorporate elements designed to capitalise upon the elucidation of the imatinib-ABL1 binding mode.<sup>17–19</sup> This was based upon the knowledge that in binding to the inactive (DFG-out) conformation of the ABL1 kinase domain,<sup>19,20</sup> the [4-(3-pyridinyl)-2-pyrimidinyl]anilino segment of imatinib had close-binding interactions with the Met318, Phe317 and Thr315 residues of the hinge-region within the ATP-binding site, but that the remaining half of the compound extended beyond the Thr315 gate-keeper residue to bind within an additional pocket. This, largely lipophilic pocket, is made accessible by the movement of the side-chain of Phe382, from its location in the DFG-in conformation where it blocks the entrance, to its position in the DFG-out conformation (Fig. 2). Consequently, the key design strategy for nilotinib was to replace the basic, polar 4-(methyloperaziny)-toluamide pharmacophore element in imatinib,<sup>16</sup> with less polar, substituted anilides, with the reasoning that the reversed-amide would maintain the H-bond interactions to Glu286 and Asp381, and, via the substituents, allow the exploration of new binding interactions.<sup>19</sup> As a consequence of this design strategy and optimisation process, although nilotinib has a similar selectivity profile to imatinib towards protein kinases, it is a more potent and selective inhibitor of ABL1 and has very few off-target activities in common with imatinib.

## 2. Methods and results

### 2.1. Comparison of nilotinib with imatinib on a structural basis

Based upon the definition of structure as the framework created by linking atoms with bonds in two-dimensions, in comparison to

imatinib, nilotinib has many different molecular structural features. The molecular similarity between these two molecules is limited to the *N*-(2-methylphenyl)-4-(3-pyridinyl)-2-pyrimidinamine moieties (depicted in black in Fig. 1). In the case of nilotinib, as assessed by summed atomic weights, this portion makes up 45% of the molecule and, in the case of imatinib, 53%. Consequently, the similarity between the two drugs may be estimated as being in the region of 50%. More refined computational assessments also reflect this lack of similarity. Based upon the systematic evaluation of structural key-type fingerprints designed to recognise molecules with similar activity,<sup>21</sup> a Tanimoto coefficient ( $T_c$ ) cut-off value of 0.7 for key-type fingerprints has been recommended as the value at which molecules identified as being 'similar' to an active compound would also be expected to be active. Using a relevant descriptor for this kind of analysis (here Daylight fingerprints) a value of 0.6 is obtained, which clearly corresponds to a degree of similarity that is well below the threshold value of 0.7 for molecular similarity.

A more pharmacophore-type descriptor (SIMILOG) was also used to assess whether other types of fingerprints would highlight the differences between the compounds given the common *N*-(2-methylphenyl)-4-(3-pyridinyl)-2-pyrimidinamine moieties. Estimating the whole molecule topological similarity between nilotinib and imatinib using the dichotomous SIMILOG descriptor,<sup>22</sup> in combination with the Tanimoto coefficient, a value of only 0.51 is obtained. To further evaluate the significance of the  $T_c$  value of 0.51, a similarity distribution for nilotinib against approximately 58,000 compounds with random biological activities from the MDL Drug Data Report (MDDR; <http://www.mdli.com>) database with similar properties (Alog *P* lipophilicity, molecular weight, number of heavy atoms, number of H-bond donors and acceptors) was generated. From this a similarity coefficient of 0.51 was achieved for approximately 2500 compounds (4.48%; Fig. 3a), a comparatively large number given the fact that these compounds were not designed to target ABL1. Extending this analysis to the Dice and Cosine metrics with similarity coefficients of 0.68 and 0.69, respectively, and correlating these values to the distributions (Fig. 3b and c) this corresponds to the relative positions of imatinib in the similarity sorted database at 4.48% and 7.47%. Thus if one were to search the MDDR database with random activities for compounds structurally similar to nilotinib, imatinib would not appear within approximately the first 2500 compounds for either Tanimoto or Dice, and not within approximately the first 4200 compounds for the Cosine coefficient. Hence, in a standard setting, they would not be selected as similar compounds. It should also be pointed out that the shape of the distributions points to the non-linear behaviour of the Tanimoto coefficient. Thus if one molecule shows a similarity value of 0.6 (dissimilarity 0.4) to a reference compound and another one a similarity value of 0.8 (dissimilarity 0.2), this does not mean that they are half as dissimilar to the reference structure, since highly similar as well as highly dissimilar structures are generally much less frequently found.

### 2.2. Comparison of nilotinib with imatinib on the basis of three-dimensional properties and interaction patterns

In terms of chemical functionality there are a number of important differences between nilotinib and imatinib (Fig. 1a–i), which result in major differences in how the two molecules interact with the kinase domain of wild-type ABL1.<sup>19</sup> As one key functionality, imatinib has a 1,3-diaminobenzene group, which is crucially important for H-bond donor interactions with the side-chains of Thr315 and Glu286 (Fig. 4), whereas in contrast nilotinib incorporates a 3-aminobenzoyl group, from which there is a hydrogen-bond donor interaction with the side-chain hydroxyl of Thr315

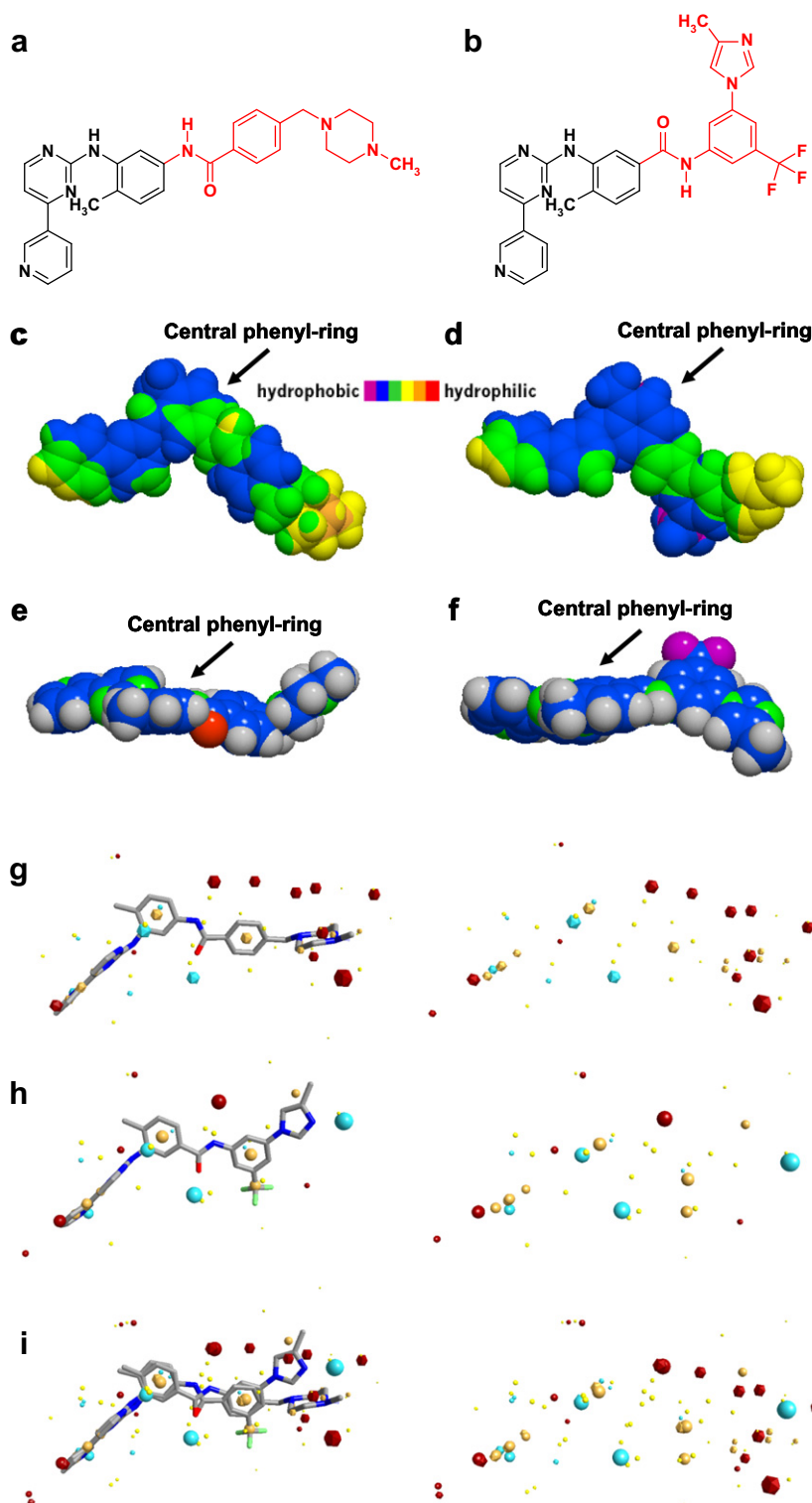


**Figure 1.** Comparison of the structural and molecular properties of (a) imatinib (Gleevec<sup>®</sup>; STI571) and (b) nilotinib (Tasigna<sup>®</sup>; AMN107); common portions of the molecules are depicted in black and the different portions in red. The 3D-structure representations depict the molecular surfaces of imatinib (c) and nilotinib (d) colour-coded according to molecular lipophilicity potential, whereas (e) and (f) show the molecular surfaces of imatinib and nilotinib, respectively, colour-coded according to atom type (carbon: blue; hydrogen: grey; nitrogen: green; oxygen: red; fluorine: magenta). The property fields for (g) imatinib (field points as spheres) and (h) nilotinib (field points as icosahedra) are overlaid in (i); negatively charged field points are displayed in cyan, positively charged points in dark-red, hydrophobic points in orange and shape points in yellow. Whereas the similar segments of the two molecules exhibit very similar field points, the remainder show very dissimilar distribution of field properties.

and a hydrogen-bond acceptor interaction with the backbone-NH of Asp381.

Imatinib also possesses a crucial 4-methyl-1-piperazine functionality, which participates in H-bond interactions with the

Ile360 and His361 of ABL, as well as imparting excellent solubility properties on the molecule. This key, highly basic, tertiary amine functionality, which is predominantly protonated in aqueous media at physiological pH, is absent in nilotinib (Table 1).

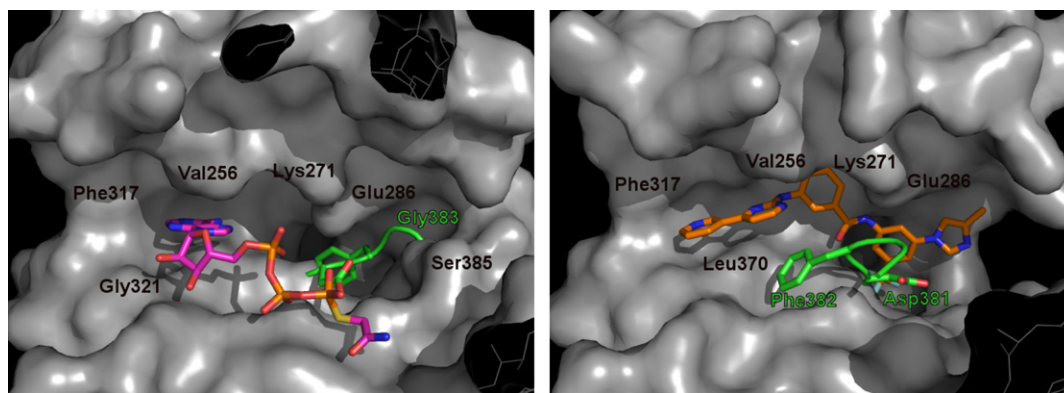


**Figure 2.** View of the ATP-binding site of ABL1 kinase with ATP bound (left, carbon atoms magenta) and with imatinib bound (right, carbon atoms orange). In both panels the solvent accessible surface of ABL1 is shown in grey, with the activation loop beyond the DFG motif (green) and the P-loop removed for clarity, as these loops cover the binding site. The DFG motif (green) is buried in the active conformation (left) and it is flipped out in the inactive conformation required for binding imatinib (right), thus lengthening the channel in which inhibitors can bind. The locations of several residues important for inhibitor binding are indicated with labels.

In contrast to imatinib, to counteract the loss of the 4-methyl-1-piperazine, a 3-methylimidazole group, as well as a trifluoromethyl group, are incorporated into the nilotinib structure, both of which make important interactions with the ABL1 kinase domain of the BCR-ABL1 protein.

In molecular recognition, a key aspect of protein–ligand binding is topological fit. Some clear differences in these topological features are illustrated in Figure 1e and f, in which blue and yellow, respectively, represent relatively hydrophobic and hydrophilic surfaces. The total polar surface area of nilotinib is 100.1 Å<sup>2</sup>, which is 16% greater than that of imatinib (Table 1). Also, as is evident from both aspects illustrated in the Figure 4, where the central phenyl ring of both nilotinib and imatinib are similarly orientated, but which differ from each other by a 90° rotation about the abscissa, the shape of nilotinib is very different from that of imatinib.

This topological dissimilarity is further highlighted using the eXtended Electron Distribution force field to compare nilotinib and imatinib in three-dimensions.<sup>23</sup> Here, different property fields (electrostatic, hydrophobic, steric, etc.) around the molecules are calculated and a similarity based upon these fields is measured. For nilotinib and imatinib the overall field similarity value is 0.664, which again shows only some degree of similarity, which is due to the *N*-(2-methylphenyl)-4-(3-pyridinyl)-2-pyrimidinamine, segment common to both molecules. The field points for imatinib, nilotinib and their overlay are depicted in Figure 1g–i, where it is evident that the western part of the fields are similar, but the variations on the eastern part of the molecules result in completely different property fields. It is these differences that are most relevant for their respective interaction specificity.

### 2.3. Comparison of imatinib and nilotinib in cellular assays for effects on kinase targets

The effects of the drugs on the phosphorylation status of the cellular targets in lysates from cells, were determined using capture enzyme linked immunosorbant assays (ELISA) as described previously for BCR-ABL1, PDGFR, KIT and DDR.<sup>11,13,24</sup> Effects of imatinib and nilotinib on CSF-1R autophosphorylation were determined in stably transfected HEK293H cells over-expressing the wild-type human CSF-1R protein, using an electrochemiluminescence assay to quantify phosphorylated CSF-1R, employing a labelled generic anti-phospho-tyrosine antibody to monitor the phosphorylation state after capture with an antibody to total receptor from the lysate.

The inhibition of BCR-ABL1, PDGFR, KIT and DDR autophosphorylation, result in the suppression of downstream signalling

from the kinases, as shown by the drug effects on cell viability.<sup>11,13,24</sup> Thus, to compare the effects of imatinib and nilotinib on the tyrosine kinase activity of BCR-ABL1 and the oncoprotein-dependent cell viability, the Philadelphia-chromosome positive human erythroleukemia K562 cell-line originally isolated from a patient with CML terminal blast crisis,<sup>25</sup> together with a murine haematopoietic Ba/F3 cell-line transfected to express human BCR-ABL1<sup>26</sup> were employed. TEL-PDGFR-β Ba/F3 cells were utilised to assess drug effects on PDGFR-dependent proliferation,<sup>27</sup> however because available antibodies were unsuitable for the ELISA, murine A31 fibroblasts stimulated with PDGF-BB were used to provide data for effects on overall PDGFR-α and -β phosphorylation.<sup>28</sup> Human GIST882 cells, expressing an activating KIT mutation (exon 13, K642E) were used to assess effects on both kinase autophosphorylation and KIT-dependent cell viability.<sup>29</sup> Otherwise transfected human embryonic kidney cells were used to quantify the inhibition of DDR and CSF-1R autophosphorylation, and a murine acute myeloid leukaemia cell-line, M-NSF-60,<sup>30</sup> dependent upon CSF for survival was used to determine drug effects on CSF-1R-dependent proliferation.

Results for the inhibition of kinase autophosphorylation and kinase dependent cell proliferation are collated in Table 2. In comparison to imatinib, nilotinib was far more potent in directly inhibiting BCR-ABL autophosphorylation and in reducing the viability of BCR-ABL dependent cell proliferation, both in murine haematopoietic Ba/F3 cells as well as in the human leukaemic K562 cell-line. Nilotinib was also more potent against DDR-1 and -2, whereas the two drugs showed similar potency against KIT, CSF-1R and both PDGFR subtypes. In terms of overall profile, imatinib shows a rank order of potency DDR-1 > PDGFR-α/β > KIT > DDR-2 > BCR-ABL1 > CSF-1R, compared to DDR-1 > DDR-2 > BCR-ABL1 > PDGFR-α/β > KIT > CSF-1R for nilotinib.

To confirm that the anti-proliferative effects were the direct result of kinase inhibition and not general cytotoxicity, imatinib and nilotinib were evaluated for their effects on parental Ba/F3 cells, cultured in the presence of interleukin-3; neither drug showed appreciable activity in this setting.

### 2.4. Comparison of adverse event profiles of nilotinib and imatinib

Nilotinib is approved in the US, European Union and many other countries worldwide for the treatment of patients with Philadelphia-chromosome positive CML in chronic and accelerated phases, who have failed prior therapy with at least one other BCR-ABL1 inhibitor including imatinib. Patients who were recruited to the



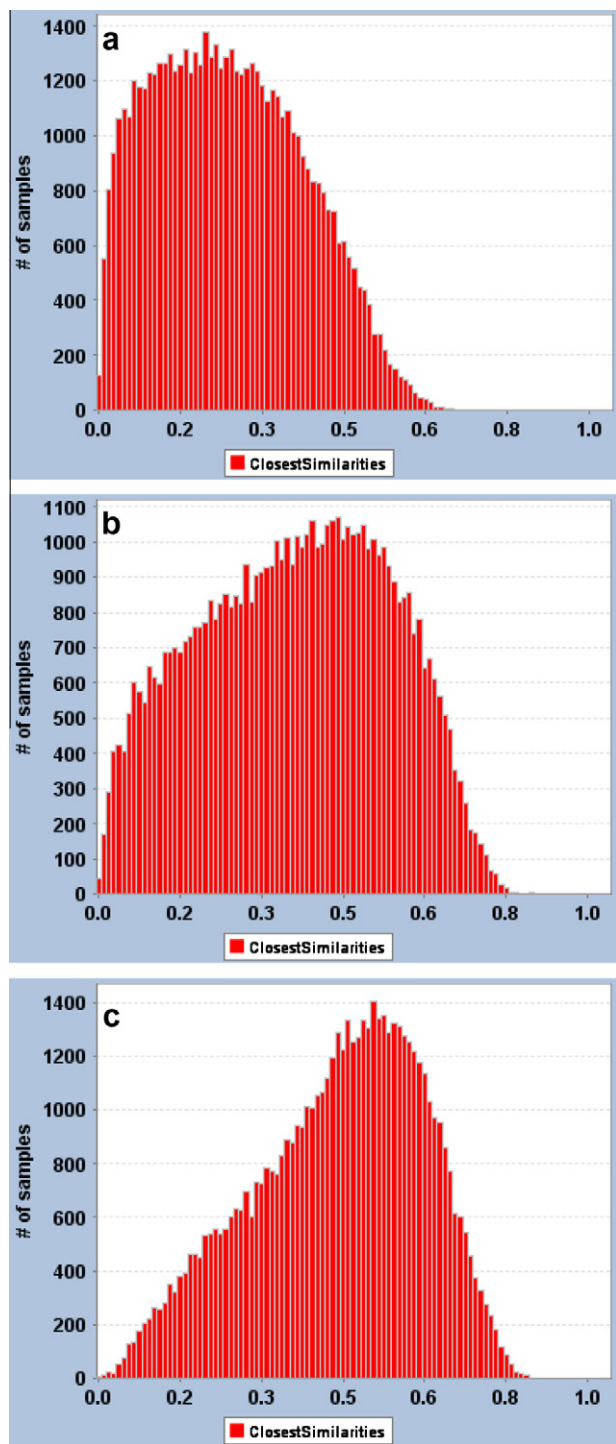


**Figure 3.** Comparison of different similarity distributions (a: Tanimoto; b: Dice; c: Cosine) of nilotinib against a sample of approximately 58,000 compounds from the MDDR compounds using the dichotomous SIMIOLOG descriptor. The y-axis describes the number of samples per similarity bin and the x-axis gives the similarity value of that bin to nilotinib. It can be clearly seen that the distributions of the Tanimoto and Dice similarities get shifted against each other, but show very similar shapes. The Cosine distribution is slightly changed, however the overall shape stays similar.

pivotal study, that resulted in regulatory Health Authority approval, were either resistant to, or intolerant of, imatinib.<sup>17</sup> Imatinib-intolerance was very strictly defined in the protocol: patients must not have achieved a major cytogenetic response (MCyR) and furthermore, only patients who had discontinued imatinib

therapy as a result of Grade 3/4 adverse events (AEs), persistent (for >1 month), or recurrent Grade 2 AEs, having recurred more than three times despite optimal supportive care, were considered to be intolerant. Of 316 patients with CML in chronic phase (CML-CP) enrolled, 95 (30%) patients were intolerant of imatinib, as a result of either non-haematologic and/or haematologic AEs. Some patients had more than one AE indicating intolerance to imatinib. Only two of 80 patients (3%) with non-haematologic imatinib-intolerance experienced a recurrence of similar intolerant symptoms during nilotinib therapy. Thirty-three patients entered the study with haematologic intolerance (neutropenia, thrombocytopenia) and only seven (21%) of these experienced similar AEs with nilotinib. Forty-seven of a total of 86 (55%) patients, who were intolerant of imatinib and who received at least 6 months of nilotinib therapy on-study, achieved MCyR. This MCyR rate is similar to that achieved in patients who were resistant to imatinib therapy.

Furthermore, in a phase I trial in patients with gastro-intestinal stromal tumours (GIST) who had failed prior therapy with imatinib and the approved second line therapy, sunitinib, the combination of imatinib 400 mg QD combined with the recommended dose of nilotinib in CML patients (400 mg BID) was found to be generally well tolerated with 16 patients remaining on therapy for over 12 months.<sup>31</sup>

These data indicate that cross-intolerance between imatinib and nilotinib is rare, representing an important therapeutic advantage for nilotinib. The lack of cross-intolerance between imatinib and nilotinib is being investigated in on-going clinical studies.

### 3. Discussion and conclusions

Measurements of indices of drug similarity are becoming increasingly important for the assessment of novelty. However, such measurements are frequently qualitative and involve subjective preconceptions. Because quantitative assessments of similarity will always be very disparate for different types of molecules and the properties concerned, the selection of the 'correct' similarity measure will always require careful consideration. The second generation CML drug, nilotinib, was rationally designed by means of structural-biology guided reengineering of the imatinib structure.<sup>16,19</sup> To the untrained eye, inspection of the two-dimensional molecular structures of imatinib and nilotinib (Fig. 1a) often leads to the opinion that the two molecules have a great resemblance to one another. However, in this study we have employed a range of algorithms to assess similarity and demonstrate that these two drugs are not very similar, either in terms of structure or their molecular properties.

The Tanimoto coefficient,  $T_c$ , is a special case of the so-called Tversky index and is generally accepted as the most appropriate distance metric for topology-based chemical similarity studies.<sup>32</sup> Given the general form of the Tversky index:

$$S(A, B) = \frac{c}{\alpha(a - c) + \beta(b - c) + c}$$

where  $a$  is the number of bits on in A,  $b$  is the number of bits on in B, and  $c$  is the number of bits on in both A and B, the Tanimoto coefficient is obtained if  $\alpha = \beta = 1$ . The same is true for the Dice coefficient where  $\alpha = \beta = 0.5$ . For binary descriptors, the Tanimoto and Dice coefficients both range from 0 (no similarity) to 1 (all bits in common). Furthermore, the Tanimoto coefficient is monotonic with the Dice coefficient.

The Cosine coefficient:

$$S(A, B) = \frac{c}{\sqrt{ab}}$$

though not monotonic with the Tanimoto coefficient, is highly correlated with it.<sup>32</sup>

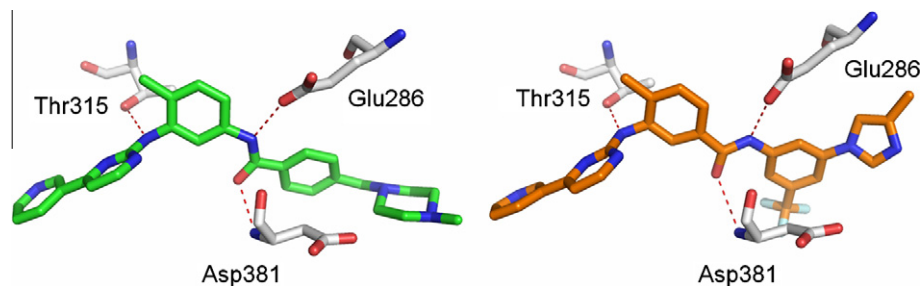


**Figure 4.** Details of the hydrogen-bonding interactions (dashed red lines) of the central regions of both inhibitors viewed from exactly the same orientation: imatinib (green, left), nilotinib (orange, right). The position of the Glu286 side chain of ABL1 kinase shifts and twists slightly to adapt to the differing positions of the NH in the amide (left) versus the reverse amide (right).

**Table 1**  
Comparison of selected physical properties of imatinib and nilotinib

	Imatinib	Nilotinib
Molecular weight (Da)	493.6	529.5
Ionisation constants: pKa1; pKa2	7.8; 3.9	5.1–5.6; 3.9
Log <i>P</i> (octanol–water)	3.1	4.9, 5.0
A log <i>P</i>	3.58	4.45
Polar surface area (Å <sup>2</sup> )	86.3	100.1
Number of H-bond acceptor sites	7	6
Number of H-bond donor sites	2	2

Ionisation constants and octanol–water partition coefficients (separate determinations) were determined by potentiometric titration and the PAMP method, respectively.<sup>64</sup> Molecular weight, Alog *P*, number of H-bond donors and acceptors was computed for the unprotonated molecules using Pipeline Pilot 7.0 (Accelrys Software Inc., San Diego, CA; <http://accelrys.com/products/scitegic>). Polar surface area was calculated using the approach of Ertl et al.<sup>65</sup>

When comparing potential algorithms for assessing similarity, such as the Tanimoto coefficient with others such as the Tversky index, Cosine and Euclidean coefficients, one has to distinguish similarity metrics by the types of data to which they are most appropriately applied. Metrics like the Tanimoto, Dice and Cosine coefficients are designed for and most typically applied to descriptors represented as vectors of binary digits (fingerprints), while the Euclidean distance is most applicable to vectors of continuous variables. Direct application of the Euclidean distance metric to fingerprint data has been demonstrated to be inferior to both the Tanimoto and Cosine metrics.<sup>33</sup> Therefore, since the Tanimoto coefficient is generally accepted as the most appropriate distance metric for fragment based chemical similarity studies, we focussed on the former in this study.

Depending upon the method of assessment, our comparison of the chemical structures of imatinib and nilotinib resulted in an estimated degree of similarity in the range of 0.5–0.6 (50–60%).

In assessing degrees of similarity using topological fingerprints and Tanimoto similarity, cut-off values for similar/dissimilar molecules are generally accepted in the literature as being between 0.85 and 0.70.<sup>34–38</sup> Bajorath has summarised some of these assessments as ‘... What *T<sub>c</sub>* (Tanimoto coefficient) threshold values should be applied to consider molecules similar on the basis of fingerprint comparison? With the introduction of the ‘neighborhood behavior’ concept, a *T<sub>c</sub>* similarity cutoff value of 0.85 was suggested because at this level, 80% of molecules identified as ‘similar’ to an active compound would also be expected to be active. However, systematic evaluation of structural key-type fingerprints designed to recognize molecules with similar activity has revealed an optimum performance at lower *T<sub>c</sub>* threshold values of approximately 0.7. ...’<sup>21</sup> Even though, this statement is based on absolute values for the similarity coefficient value, we believe that a value of 0.5–0.6 is an indication of a lack of similarity. This conclusion is further supported by the relative comparison with the random set of drug-like molecules in the MDDR database. Here, for all similarity coefficients employed (Tanimoto, Dice, Cosine), imatinib would have not been selected as similar to nilotinib in a standard setting of similarity searching. However, as discussed by Flower,<sup>36</sup> numerical assessments of similarity will vary depending upon the descriptors employed and can lead to divergent conclusions. Consequently in this study, orthogonal descriptors commonly used within standard research environments were employed for the analysis and these are to some extent validated in that the structural differences lead to crucial differences in both the macroscopic properties and the biological activities of the two drugs. In the case of the former, some key physicochemical properties are compared in Table 2. Thus the presence of the *N*-methylpiperidine group renders imatinib a relatively strong organic base (pKa1 7.7; pKa2 3.9), such that it is highly protonated on the methylated piperidine-*N* at physiological pH,<sup>39</sup> and consequently highly soluble at pH <5.5. In contrast, nilotinib

**Table 2**  
Comparison of effects of imatinib and nilotinib on principal kinase targets (n.d.: not determined)

Kinase	Cell-line	Imatinib		Nilotinib	
		Kinase Inhibition Mean IC <sub>50</sub> ± SEM (nM)	Cell Proliferation	Kinase Inhibition Mean IC <sub>50</sub> ± SEM (nM)	Cell Proliferation
BCR-ABL1	K562	473 ± 60 (n = 15)	244 ± 14 (n = 43)	42 ± 8 (n = 5)	21 ± 9 (n = 62)
BCR-ABL1	BCR-ABL1 transfected Ba/F3	221 ± 31 (n = 14)	678 ± 39 (n = 23)	20 ± 2 (n = 7)	25 ± 7 (n = 68)
PDGFR-α and -β	A31	72 ± 10 (n = 12)	n.d.	71 ± 5 (n = 81)	n.d.
PDGFR-β	TEL-PDGFR-β transfected Ba/F3	n.d.	39 ± 4 (n = 8)	n.d.	62 ± 8 (n = 14)
KIT	GIST882	97 ± 12 (n = 7)	108 ± 7 (n = 13)	217 ± 8 (n = 80)	151 ± 8 (n = 29)
DDR-1	DDR-1 transfected HEK393	43 ± 2.4 (n = 4)	n.d.	3.7 ± 1.2 (n = 4)	n.d.
DDR-2	DDR-2 transfected HEK393	141 ± 33 (n = 3)	n.d.	5.2 ± 3.3 (n = 3)	n.d.
CSF-1R	CSF-1R transfected HEK293	291 ± 54 (n = 5)	n.d.	677 ± 437 (n = 7)	n.d.
CSF-1R	M-NFS-60	n.d.	358 ± 101 (n = 3)	n.d.	838 ± 425 (n = 3)
Parental Ba/F3 cells + interleukin 3		n.d.	9459 ± 1931 (n = 3)	n.d.	>10,000 (n = 71)

is much less basic ( $pK_{a1}$  5.1–5.6;  $pK_{a2}$  3.9) and is highly lipophilic (Table 1), so that it is not highly protonated under physiological conditions and only shows appreciable aqueous solubility at pH <2.

The differences in molecular structure and in physicochemical properties combine to result in significant differences in the in vitro and in vivo pharmacological properties of the two drugs, which is evident upon comparing their effects on biological targets in cellular assays.

The difference in basicity between the two compounds is manifested in the different cell-transport properties of imatinib and nilotinib. Imatinib is a substrate for the oxycation transporter, hOCT1 and the P-glycoprotein transporter (Pgp or MDR1; encoded by the *ABCB1* gene).<sup>40–42</sup> Three hOCT proteins are expressed in man, which serve as bidirectional transporters of organic cations across cell membranes. The hOCT1 transporter is of particular importance for the transport of imatinib into CML cells as shown by the correlations between patient responses and the level of hOCT1 activity in their peripheral blood mononuclear cells.<sup>43,44</sup> As a weak base, nilotinib is not highly ionised at physiological pH and it is transported into cells primarily through passive diffusion and consequently is independent of hOCT1 transporter activity.<sup>41,45</sup> Nilotinib is therefore likely to show efficacy in patients whose response to imatinib is compromised by low hOCT1 activity. It is also well established the Pgp transporter plays a major role in the cell efflux of imatinib and it has also been recently demonstrated that nilotinib is not a substrate for this transporter, indicating that differential expression and/or function of Pgp is unlikely to affect nilotinib cellular disposition.<sup>42</sup>

The differences in molecular structure also impact the pharmacophores of imatinib and nilotinib. The molecular interactions which are responsible for the binding of both drugs to BCR-ABL1 have been revealed by the crystal structures of the drugs in complex with the ABL1 tyrosine kinase domain.<sup>11,17–19</sup> Furthermore, NMR studies of the drug-complexes, have shown that in solution the drugs bind to ABL1 in a similar fashion to that observed by X-ray crystallography.<sup>46</sup> Consistent with the design principle employed for the compound series that lead to the discovery of nilotinib, the manner in which imatinib and nilotinib form hydrogen-bonds to Glu286 and Asp381, and occupy the lipophilic pocket are very different. Clearly the different H-bonding pattern results from the replacement of the benzanilide group in imatinib with the benzamide in nilotinib. However, whereas the bifurcated H-bonding between Ile360 and His361 of ABL1 and the *N*-methylpiperazine governs the docking of imatinib, nilotinib binds through a large number of weak interactions arising from van der Waals contacts. This assembly of weak interactions would not occur were it not for the excellent topological fit of nilotinib within the binding site (Fig. 5), with the improved fit stemming from the differences in the electrostatic, hydrophobic and steric fields surrounding the two molecules.

The differences in binding to kinase domains, such as that of ABL1, translate into the drugs having different kinase selectivity profiles. Although kinase profiles are often discussed in terms of activities in biochemical assays, employing kinase domain constructs with artificial substrates and short incubation times, more pertinent data are generated in cellular assays with full length proteins, where activity can be correlated with effects on kinase-dependent cell viability in proliferation assays.<sup>13</sup>

Four molecular targets are validated for imatinib in that the drug shows clinical efficacy in the treatment of CML,<sup>8</sup> gastrointestinal stromal tumours (GIST),<sup>47</sup> chronic myelomonocytic leukaemia (CCML),<sup>48</sup> and pigmented villonodular synovitis (PVNS),<sup>49</sup> as a consequence of inhibiting BCR-ABL1, and the receptor kinases for stem cell factor (KIT), platelet-derived growth factor (TEL-PDGFR $\beta$ ) and colony stimulating factor (CSF-1R), respectively, at physiologically relevant concentrations.<sup>50</sup> In addition, imatinib is

a potent inhibitor of the collagen-activated, discoidin domain receptor kinases DDR-1 and -2,<sup>24,51</sup> although at the current time no therapeutic applications or pharmacological effects have been identified stemming from this activity.

From the comparison of the effects of imatinib and nilotinib as tyrosine kinase inhibitors (Table 2), although they have similar target profiles their selectivity profiles are quite different, as reflected in the different rank-orders of activity, with nilotinib being much more potent and selective towards BCR-ABL1. This is important, since degree of selectivity of kinase inhibitors is central to the concept of targeted cancer therapy. Thus, whereas cytotoxic chemotherapies usually impact all rapidly dividing cells, such that in a large patient population they frequently achieve little patient benefit at the price of high toxicity, targeted drugs aim to achieve high patient benefit in smaller patient populations that are homogenous with regard to expressing the molecular target of the drug and, in the absence of off-target liabilities, should be better tolerated. In the case of CML, the tyrosine kinase activity of the BCR-ABL1 oncoprotein is clearly established as being the relevant drug target, and imatinib is widely accepted as being the first targeted cancer therapy. However, despite the great benefit derived from this drug, many CML patients experience side-effects and show poor adherence to their prescribed regimen,<sup>52</sup> or even have to discontinue therapy due to tolerability issues,<sup>53</sup> thus highlighting the need to minimise off-target effects of such drugs when used as long-term chronic therapies.

When translating in vitro cellular selectivity profiles of drugs into adverse-event liabilities, it is important to consider drug-exposure levels in patients following therapeutic doses, since side-effects can also be limited by insufficient target inhibition in the relevant organs. At standard doses, imatinib (400 mg q24h) and nilotinib (400 mg q12h) achieve steady-state trough concentrations of 1.98 and 1.95  $\mu$ M, respectively,<sup>50,54</sup> and neither drug significantly penetrates the blood–brain-barrier. Consequently, other than the differences in transporter expression referred to above, pharmacodynamic differences are unlikely to play a major role in discriminating between imatinib and nilotinib. Therefore, the high potency and selectivity of nilotinib towards BCR-ABL1, probably responsible for the tolerability of the drug, its superior efficacy in the treatment of newly diagnosed CML patients,<sup>53,55</sup> and its efficacy in the treatment of imatinib-resistant patients not carrying imatinib-resistant BCR-ABL1 mutations.<sup>14,15</sup>

The differences in the safety and tolerability profiles of the two drugs in patients is particularly evident in the lack of cross-intolerance in patients who failed prior therapy with imatinib and have subsequently been treated with nilotinib. The more severe adverse events leading to intolerance are therefore probably attributable to off-target effects and, in the absence of non-kinase targets other than the NQO2 oxidoreductase and carbonic anhydrase enzymes, which both drugs have been reported to inhibit in biochemical assays,<sup>51,56</sup> it seems likely that these might result from the different kinase selectivities, combined with differences in pharmacodynamic properties. Notable among the differences in adverse events is the lack of fluid retention seen with nilotinib treatment, particularly since this relatively common imatinib side-effect has been linked to PDGFR inhibition, which both drugs potentially inhibit to a similar extent (Table 3).<sup>57</sup> Based upon this finding, the role of PDGFR in imatinib-induced fluid retention is brought into question and, since imatinib-like, periorbital oedema has recently been reported to be a side-effect of the CSF-1 antibody PD-0360324,<sup>58</sup> it can be speculated that inhibition of this kinase might be involved in the fluid retention seen with imatinib.

In conclusion, the approaches employed in this manuscript illustrate a strategy to compare the structures of two molecules and provide supporting data regarding relevant properties which support the degree of similarity. The Daylight/Tanimoto similarity

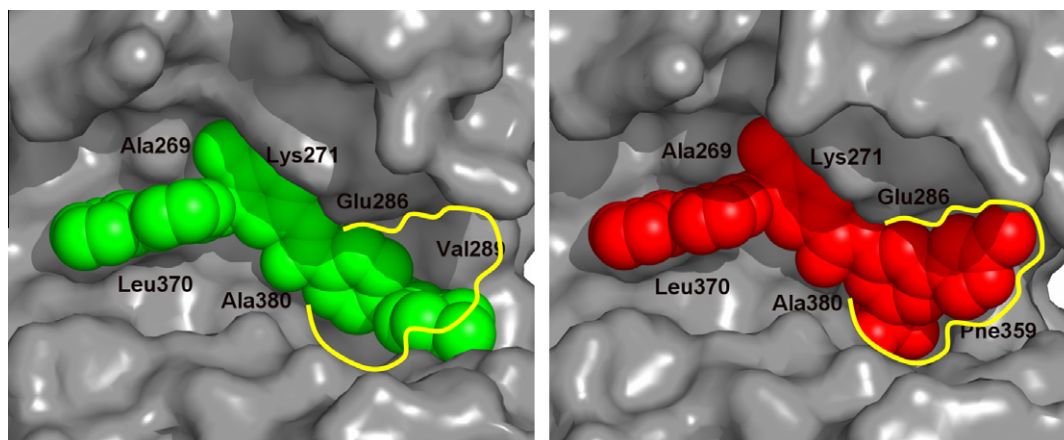


**Figure 5.** Comparison of the binding surfaces of ABL1 kinase with imatinib bound (green, left) and nilotinib bound (red, right). In both pictures the solvent accessible surface of ABL1 is shown in grey with the P-loop and part of the activation loop removed for clarity (as in Fig. 2). The yellow line outlines the cavity created by the shift of the DFG-motif from the DFG-in or active position, to the DFG-out position required for the binding of imatinib or nilotinib. The locations of several residues important for inhibitor binding are indicated with labels.

**Table 3**  
Imatinib and nilotinib cross intolerance in chronic and accelerated phase CML (same non-haematologic adverse events (AE) that occurred in the same patient during both imatinib and nilotinib therapy)

Reason for imatinib-intolerance	Chronic phase CML <i>n</i> = 94		Accelerated phase CML <i>n</i> = 23	
	Imatinib intolerant, <i>n</i>	Grade 3/4 on nilotinib, <i>n</i>	Imatinib intolerant, <i>n</i>	Grade 3/4 on nilotinib, <i>n</i>
Fluid retention	17	0	5	0
GI intolerance	16	1	1	0
Liver toxicity	10	1	3	0
Alanine transaminase (ALT)	4	0	1	0
Aspartate aminotransferase (AST)	4	1	0	0
Liver function test (LFT) abnormal	1	0	0	0
Myalgia/arthritis	9	0	1	0
Rash/skin toxicity	26	0	5	0

value of 0.6 for imatinib and nilotinib, clearly corresponds to a degree of similarity that is well below the generally recognised threshold value of 0.7 for molecular similarity. Furthermore, the structural differences are reflected in substantial differences in the physicochemical and pharmacodynamic properties of the drugs and, manifested in patients in different side-effect profiles as reflected in the marked lack of cross-intolerance. This analysis of imatinib and nilotinib formed the basis of a report, using the criteria to assess the structural similarity of the compounds as outlined in the European Commission Communication (C(2008) 4077 final, 19 Sep 2008) for assessing similarity of medicinal products versus authorised orphan drugs benefiting from market exclusivity,<sup>2</sup> which concluded that nilotinib had a low degree of structural resemblance to imatinib. However, the arguments put forward were not upheld in the assessment given by the CHMP, who concluded that both molecules share the same principal molecular structural features rendering half of the molecules identical and, if a molecule is 50% identical with the possibility of even more additional similarity, this is considered enough to conclude structural similarity. Borrowing from a treatise from Hans-Jörg Roth,<sup>59</sup> these two different conclusions regarding similarity are probably related to different frames of reference being employed in the two assessments and illustrate the difficulty of applying the concept of similarity in an absolute sense. Since there is no obvious solution to the absolute similarity problem, we have presented a method to assess the similarity coefficient between two

molecules within a suitable frame of reference using similarity distributions of drug-like molecules with similar overall properties. This procedure is similar in spirit to a hypothesis test, whereby one evaluates whether or not a molecule/observation of interest lies within the noise of the background molecules/observations. The importance of these structural differences is highlighted in how they translate into the greatly enhanced potency and selectivity of nilotinib towards the tyrosine kinase activity of BCR-ABL1, which is reflected in the efficacy of this drug as a treatment for CML, with a favourable side-effect profile.

## 4. Experimental section

### 4.1. Computational chemistry

Structural comparisons were performed based upon the conformations as found in the corresponding ligand–protein crystal structures (PDB entry 3CS9 for nilotinib and 2HYY for imatinib). Based upon these conformations, eXtended Electron Distribution force field similarity values,<sup>23</sup> together with topological similarity measures by means of SIMIOLOG keys and Daylight fingerprints (as example of a structural ‘key-type’ fingerprint),<sup>22</sup> in combination with the Tanimoto coefficient ( $T_c$ ),<sup>60</sup> were calculated.

Database comparisons were done for compounds from the MDL Drug Data Report (MDDR; <http://www.mdli.com>) database with similar properties (Alog *P*, molecular weight, number of heavy



atoms, number of H-bond donors and acceptors, Table 1). These properties were calculated using the PipelinePilot software package. To have a reasonably large reference set of compounds, a subset of 58,000 compounds were selected.

## 4.2. Materials

Imatinib (4-[(4-methyl-1-piperazinyl)methyl]-N-[4-methyl-3-[[4-(3-pyridinyl)-2-pyrimidinyl]amino]phenyl]-benzamide) and nilotinib (4-methyl-N-[3-(4-methyl-1H-imidazol-1-yl)-5-(trifluoromethyl)phenyl]-3-[[4-(3-pyridinyl)-2-pyrimidinyl]amino]benzamide) were synthesised as described previously.<sup>6,10</sup> The erythroleukemia cell-line K562, derived from a patient in blast crisis CML, was purchased from American Type Culture Collection (Rockville, MD; ATCC Cat. CCL-243). Ba/F3-BCR-ABL1 cells were obtained by transfecting the interleukin-3-dependent murine hematopoietic Ba/F3 cell line with a pGD vector containing *wild-type* (p210 kD) BCR-ABL1 (B2A2) cDNA.<sup>26,61,62</sup> BALB/c 3T3 A31 mouse embryonic fibroblasts (ATCC Cat. CCL-163), expressing PDGFR- $\alpha$  and - $\beta$  were obtained from B.J. Druker (Univ. Oregon, Portland, USA). BaF3-Tel-PDGFR $\beta$ ,<sup>28</sup> transduced with a fusion protein comprised of the dimerising portion of TEL and the transmembrane and kinase domain of the PDGFR $\beta$ ,<sup>63</sup> were provided by G. Gilliland (Brigham and Women's Hospital and Harvard Medical School, Boston, USA). GIST882, a human gastrointestinal stromal tumour (GIST) cell line expressing an activating KIT mutation (exon 13, K642E) was provided by J. Fletcher (MIT Cancer Center and Department of Biology, Cambridge).<sup>29</sup> HEK293-DDR-1 and HEK293-DDR-2 cells were obtained as described previously.<sup>24</sup>

A stable cell line over-expressing *wild-type* human CSF-1R was generated from human embryonic kidney cells (HEK293H, Gibco), using an expression plasmid generated by subcloning full-length CSF-1R cDNA (Entrez: NM\_005211.2) into the commercial vector pcDNA3.1/hygro/lacZ (Invitrogen) adapted for gateway cloning; the cells were maintained in DMEM + 10% FBS with added Na pyruvate and antibiotics and under hygromycin selection of 50  $\mu$ g/mL. The M-CSF dependent, murine myeloblastic M-NSF-60 cell-line was obtained from American Type Culture Collection (Rockville, MD; CRL-1838).

## 4.3. Cellular autophosphorylation assays

The phosphorylation status of BCR-ABL1, PDGFR, KIT and DDR-1 and -2, in lysates from cells in the presence or absence of drug, was determined with capture ELISAs as described previously.<sup>11,13,24,28</sup>

A clone of HEK293H cells stably expressing the *wild-type* CSF-1R receptor was used to determine the effects of imatinib and nilotinib on CSF-1R autophosphorylation. A capture immunosorbant assay was developed using the electrochemiluminescence (ECL) technology from Meso Scale Discovery (MSD). A polyclonal antibody specific to CSF-1 (cfms; Santa Cruz Biotechnology, Cat. SC692) was used to coat small spot ECL plates (MSD) using 0.5  $\mu$ L per well of a 1  $\mu$ M solution of Ab in PBS. Prior to use, plates were blocked with a solution of 3% BSA. Cells maintained in DMEM supplemented with 10% FBS and 50  $\mu$ g/mL Hygromycin B were seeded at 15,000–20,000 per well into Poly-D-Lysine plates (Greiner Bio-One, Cat. 655940) 1 day before assay. Test compounds were serially diluted in DMSO, then into complete culture media before incubation with cells for 90 min. After stimulation by the addition of 50 ng/mL of human M-CSF (R&D Systems, Cat. 216-MC) for 5–10 min, culture supernatants were removed and cells were lysed by the addition of 50  $\mu$ L ice-cold lysis buffer (20 mM Tris/HCl, pH 7.5, 150 mM NaCl, 1 mM EDTA, 1 mM EGTA, 1% Triton-X-100, phosphatase and protease inhibitors). For detection of CSF-1R phosphorylation, 25  $\mu$ L of lysates were transferred to the spotted

and blocked ECL plates and incubated overnight at 4 °C with shaking. Phosphorylation of the captured targets was detected using a commercial anti-P-Tyr Ab labelled with SULFO-tag (PY20, Cat. R32AP) and quantified using 1.5 $\times$  Read T Buffer (Cat. R93TC) on a Sector 6000 instrument (all, MSD).

## 4.4. CSF-1R dependent cellular proliferation

To determine the effects of imatinib and nilotinib on cell viability and proliferation due to inhibition of CSF-1R phosphorylation, M-NFS-60, a murine AML cell-line dependent on M-CSF for growth and survival was used. Cells were washed prior to seeding into black-walled tissue culture plates (Nunc) at 50,000 cells per well in 50  $\mu$ L complete growth medium (RPMI, 10% FBS, 30 ng/mL M-CSF). An additional 50  $\mu$ L of complete medium containing serial dilutions of test compounds was added and incubated for 72 h (37 °C, 5% CO<sub>2</sub>). Cells treated with equivalent DMSO were used as a positive growth control and cells without M-CSF as a no growth control. Cell growth was assessed using a luminescent cell viability assay kit (CellTiter-Glo, Promega) to measure the amount of ATP present in a well after lysis of the cells. After incubation, cells were brought to room temperature and 100  $\mu$ L of CellTiter-Glo<sup>®</sup> reagent (mixed from kit components) added to the 100  $\mu$ L cells in each well. Plates were shaken for 2 min and incubated at room temperature for 10 min prior to reading luminescence on a Perkin Elmer Trilux instrument. The ATP released upon lysis is used in an enzymatic reaction which includes Luciferase and its substrate Luciferin. The amount of light emitted is proportional to the amount of ATP, which in turn is proportional to the number of live cells in the well.

For both the CSF-1R phosphorylation and the cell proliferation assays, IC<sub>50</sub> values were determined from the dose response curves by graphical extrapolation.

## 4.5. Patient cross-intolerance

Imatinib intolerant-patients (107) were part of a phase II open-label study evaluating the efficacy, safety and tolerability of nilotinib in subjects (447) with imatinib-resistant or imatinib-intolerant CML.<sup>17</sup> Imatinib-intolerance was defined as not achieving a major cytogenetic response and the discontinuation of imatinib therapy due to Grade 3/4 adverse events or Grade 2 adverse events that either persisted for more than 1 month, or recurred >3 times despite optimal supportive care. Some patients had more than one adverse event (AE) meeting the criteria for intolerance. Approximately 75% of the imatinib-intolerant patients discontinued imatinib due to Grade 3/4 adverse events. Cross-intolerance was defined as the occurrence of the same Grade 3/4 nilotinib toxicity or Grade 2 nilotinib toxicity that persisted longer than 1 month, regardless of causality, that had led to discontinuation of imatinib therapy.

## References and notes

- Saliner, A. G. *Curr. Comput. Aided Drug Des.* **2006**, *2*, 105.
- Guideline on aspects of the application of Article 8(1) and (3) of Regulation (EC) No 141/2000: assessing similarity of medicinal products versus authorised orphan medicinal products benefiting from market exclusivity and applying derogations from that market exclusivity. *Official J. Eur. Union* **2008**, C242, 12.
- Commission Regulation (EC) No 847/2000 of 27 April 2000 laying down the provisions for implementation of the criteria for designation of a medicinal product as an orphan medicinal product and definitions of the concepts 'similar medicinal product' and 'clinical superiority'. *Official J. Eur. Union* **2000**, L103, 5.
- Communication from the Commission. Guideline on aspects of the application of Article 8(1) and (3) of Regulation (EC) No 141/2000: assessing similarity of medicinal products versus authorised orphan medicinal products benefiting from market exclusivity and applying derogations from that market exclusivity.
- Melo, J. V.; Barnes, D. J. *Nat. Rev. Cancer* **2007**, *7*, 441.
- Zimmermann, J. Pyrimidinderivate und Verfahren zu ihrer Herstellung. *Eur. Pat. Appl.* 564,409, March 25, 1993.

7. Zimmermann, J.; Buchdunger, E.; Mett, H.; Meyer, T.; Lydon, N. B. *Bioorg. Med. Chem. Lett.* **1997**, 7, 187.
8. Hochhaus, A.; Druker, B.; Sawyers, C.; Guilhot, F.; Schiffer, C. A.; Cortes, J.; Niederwieser, D. W.; Gambacorti, C.; Stone, R. M.; Goldman, J.; Fischer, T.; O'Brien, S. G.; Reiffers, J. J.; Mone, M.; Krahnke, T.; Talpaz, M.; Kantarjian, H. M. *Blood* **2008**, 111, 1039.
9. Apperley, J. F. *Lancet Oncol.* **2007**, 8, 1018.
10. Breitenstein, W.; Furet, P.; Jacob, S.; Manley, P. W. Preparation of pyrimidinylaminobenzamides as inhibitors of protein kinases, in particular tyrosine kinases for treating neoplasm, especially leukemia. PCT Int. Appl. WO 2004005281, Jan 15, 2004.
11. Weisberg, E.; Manley, P. W.; Breitenstein, W.; Brügggen, J.; Cowan-Jacob, S. W.; Ray, A.; Huntly, B.; Fabbro, D.; Fendrich, G.; Hall-Meyers, E.; Kung, A. L.; Mestan, J.; Daley, G. Q.; Callahan, L.; Catley, L.; Cavazza, C.; Mohammed, A.; Neuberg, D.; Wright, R. D.; Gilliland, D. G.; Griffin, D. G. *Cancer Cell* **2005**, 7, 129.
12. Weisberg, E.; Manley, P.; Mestan, J.; Cowan-Jacob, S.; Ray, A.; Griffin, J. D. *Br. J. Cancer* **2006**, 94, 1765.
13. Manley, P. W.; Druce, P.; Fendrich, G.; Furet, P.; Liebetanz, J.; Martiny-Baron, G.; Mestan, J.; Trappe, J.; Wartmann, M.; Fabbro, D. *Biochim. Biophys. Acta* **2010**, 1804, 445.
14. Kantarjian, H. M.; Giles, F.; Gattermann, N.; Bhalla, K.; Alimena, G.; Palandri, F.; Ossenkoppele, G. J.; Nicolini, F.-E.; O'Brien, S. G.; Litow, M.; Bhatia, R.; Cervantes, F.; Haque, A.; Shou, Y.; Resta, D. J.; Weitzman, A.; Hochhaus, A.; le Coutre, P. *Blood* **2007**, 110, 3540.
15. le Coutre, P.; Ottmann, O. G.; Giles, F.; Kim, D.-W.; Cortes, J.; Gattermann, N.; Apperley, J. F.; Larson, R. A.; Abruzzese, E.; O'Brien, S. G.; Kuliczowski, K.; Hochhaus, A.; Mahon, F.-X.; Saglio, G.; Gobbi, M.; Kwong, Y.-L.; Baccarani, M.; Hughes, T.; Martinelli, G.; Radich, J. P.; Zheng, M.; Shou, Y.; Kantarjian, H. *Blood* **2008**, 111, 1834.
16. Manley, P. W.; Breitenstein, W.; Brügggen, J.; Cowan-Jacob, S. W.; Furet, P.; Mestan, J.; Meyer, T. *Bioorg. Med. Chem. Lett.* **2004**, 14, 5793.
17. Nagar, B.; Bornmann, W. G.; Pellicena, P.; Schindler, T.; Veach, D. R.; Miller, W. T.; Clarkson, B.; Kuriyan, J. *Cancer Res.* **2002**, 62, 4236.
18. Manley, P. W.; Cowan-Jacob, S. W.; Buchdunger, E.; Fabbro, D.; Fendrich, G.; Furet, P.; Meyer, T.; Zimmermann, J. *Eur. J. Cancer* **2002**, 38, S19.
19. Cowan-Jacob, S. W.; Fendrich, G.; Floersheimer, A.; Furet, P.; Liebetanz, J.; Rummel, G.; Rheinberger, P.; Centeleghe, M.; Fabbro, D.; Manley, P. W. *Acta Crystallogr. D Biol. Crystallogr.* **2007**, 63, 80.
20. Cowan-Jacob, S. W.; Guez, V.; Fendrich, G.; Griffin, J. D.; Fabbro, D.; Furet, P.; Liebetanz, J.; Mestan, J.; Manley, P. W. *Mini-Rev. Med. Chem.* **2004**, 4, 285.
21. Bajorath, J. *Chem. Inf. Comput. Sci.* **2001**, 41, 233.
22. Schuffenhauer, A.; Floersheim, P.; Acklin, P.; Jacoby, E. J. *Chem. Inf. Comput. Sci.* **2003**, 43, 391.
23. Cheeseright, T.; Mackey, M.; Rose, S.; Vinter, A. J. *Chem. Inf. Model.* **2006**, 46, 665.
24. Day, E.; Waters, B.; Spiegel, K.; Alnadaf, T.; Manley, P. W.; Buchdunger, E.; Walker, C.; Jarai, G. *Eur. J. Pharmacol.* **2008**, 599, 44.
25. Luzzio, C. B.; Luzzio, B. B. *Blood* **1975**, 45, 321.
26. Daley, G. O.; Baltimore, D. *Proc. Natl. Acad. Sci.* **1988**, 85, 9312.
27. Carroll, M.; Tomasson, M. H.; Barker, G. F.; Golub, T. R.; Gilliland, D. G. *Proc. Natl. Acad. Sci.* **1996**, 93, 14845.
28. Manley, P. W.; Mestan, J.; Meyer, T.; Fabbro, D. *Proceedings of the 97th Annual Meeting of the American Association for Cancer Research*, Apr 1–5, 2006; AACR: Washington, DC, Philadelphia (PA), 2006; p 7. Abstr. 30.
29. Tuveson, D. A.; Willis, N. A.; Jacks, T.; Griffin, J. D.; Singer, S.; Fletcher, C. D.; Fletcher, J. A.; Demetri, G. D. *Oncogene* **2001**, 20, 5054.
30. Nakoinz, I.; Lee, M.-T.; Weaver, J. F.; Ralph, P. J. *Immunol.* **1990**, 145, 860.
31. Demetri, G. D.; Casali, P. G.; Blay, J.-Y.; von Mehren, M.; Morgan, J. A.; Bertulli, R.; Ray-Coquard, I.; Cassier, P.; Davey, M.; Borghaei, H.; Pink, D.; Debiec-Rychter, M.; Cheung, W.; Bailey, S. M.; Veronese, M. L.; Reichardt, A.; Fumagalli, E.; Reichardt, P. *Clin. Cancer Res.* **2009**, 15, 5910.
32. Willett, P.; Barnard, J. M.; Downs, G. M. J. *Chem. Inf. Comput. Sci.* **1998**, 38, 983.
33. Willett, P.; Winterman, V. *Quant. Struct.-Act. Relat.* **1986**, 5, 18.
34. Delaney, J. S. *Mol. Divers.* **1996**, 1, 217.
35. Brown, R. D.; Martin, Y. C. *SAR QSAR Environ. Res.* **1998**, 8, 23.
36. Flower, D. R. *J. Chem. Inf. Comput. Sci.* **1998**, 38, 379.
37. Xue, L.; Godden, J.; Bajorath, J. *J. Chem. Inf. Comput. Sci.* **1999**, 39, 881.
38. Martin, Y. C.; Kofron, J. L.; Traphagen, L. M. *J. Med. Chem.* **2002**, 45, 4350.
39. Szakács, Z.; Béni, S.; Varga, Z.; Örfi, L.; Kéri, G.; Noszá, B. *J. Med. Chem.* **2005**, 48, 249.
40. Thomas, J.; Wang, L.; Clark, R. E.; Pirmohamed, M. *Blood* **2004**, 104, 3739.
41. White, D. L.; Saunders, V. A.; Dang, P.; Engler, J.; Zannettino, A. C.; Cambareri, A. C.; Quinn, S. R.; Manley, P. W.; Hughes, T. P. *Blood* **2006**, 108, 697.
42. Haouala, A.; Rumpold, H.; Untergasser, G.; Buclin, T.; Ris, H.-B.; Widmer, N.; Decosterd, L. A. *Drug Met. Lett.* **2010**, 4, 114.
43. Wang, L.; Giannoudis, A.; Lane, S.; Williamson, P.; Pirmohamed, M.; Clark, R. E. *Clin. Pharmacol. Ther.* **2008**, 83, 258.
44. White, D. L.; Dang, P.; Engler, J.; Venables, A.; Zrim, S.; Osborn, M.; Saunders, V. A.; Manley, P. W.; Hughes, T. P. *J. Clin. Oncol.* **2010**, 28, 2761.
45. Davies, A.; Jordanides, N. E.; Giannoudis, A.; Lucas, C. M.; Hatzieremia, S.; Harris, R. J.; Jørgensen, R. E.; Holyoake, T. L.; Pirmohamed, M.; Clark, R. E.; Mountford, J. C. *Leukemia* **2009**, 23, 1999.
46. Vajpai, N.; Strauss, A.; Fendrich, G.; Cowan-Jacob, S. W.; Manley, P. W.; Gzesiek, S.; Jahnke, W. J. *Biol. Chem.* **2008**, 283, 18292.
47. Blanke, C. D.; Rankin, C.; Demetri, G. D.; Ryan, C. W.; von Mehren, M.; Benjamin, R. S.; Raymond, A. K.; Bramwell, V. H. C.; Baker, L. H.; Maki, R. G.; Tanaka, M.; Hecht, J. R.; Heinrich, M. C.; Fletcher, C. D. M.; Crowley, J. J.; Borden, E. C. *J. Clin. Oncol.* **2008**, 26, 626.
48. Apperley, J. F.; Gardembas, M.; Melo, J. V.; Russell-Jones, R.; Bain, B. J.; Baxter, E. J.; Chase, A.; Chessells, J. M.; Colombat, M.; Dearden, C. E.; Dimitrijevic, S.; Mahon, F.-X.; Marin, D.; Nikolova, Z.; Olavarria, E.; Silberman, S.; Schultheis, B.; Cross, N. C. P.; Goldman, J. M. N. *Engl. J. Med.* **2002**, 347, 481.
49. Blaye, J.-Y.; El Sayadi, H.; Thiesse, P.; Garret, J.; Ray-Coquard, I. *Ann. Oncol.* **2008**, 19, 821.
50. Larson, R. A.; Druker, B. J.; Guilhot, F.; O'Brien, G. G.; Riviere, G. J.; Krahnke, T.; Gathmann, I.; Wang, Y. *Blood* **2008**, 111, 4022.
51. Rix, U.; Hantschel, O.; Dürnberger, G.; Remsing Rix, L. L.; Planysavsky, M.; Fernbach, N. V.; Kaup, I.; Bennett, K. L.; Valent, P.; Colinge, J.; Köcher, T.; Superti-Furga, G. *Blood* **2007**, 110, 4055.
52. Marin, D.; Bazeos, A.; Mahon, F.-X.; Eliasson, L.; Milojkovic, D.; Bua, M.; Apperley, J. F.; Szydlo, R.; Desai, R.; Kozlowski, K.; Paliompeis, C.; Latham, V.; Foroni, L.; Molimard, M.; Reid, A.; Rezvani, K.; de Lavallade, H.; Guallar, C.; Goldman, J.; Khorashad, J. S. *J. Clin. Oncol.* **2010**, 28, 2381.
53. Cortes, J. E.; Jones, D.; O'Brien, S.; Jabbour, E.; Konopleva, M.; Ferrajoli, A.; Tapan Kadia, T.; Borthakur, G.; Stigliano, D.; Shan, J.; Kantarjian, H. *J. Clin. Oncol.* **2010**, 28, 392.
54. Tanaka, C.; Yin, O.; Sethuraman, V.; Smith, T.; Wang, X. F.; Grouss, K.; Kantarjian, H.; Giles, F.; Ottmann, O. G.; Galitz, L.; Schran, H. *Clin. Pharmacol. Ther.* **2010**, 87, 197.
55. Saglio, G.; Kim, D.-W.; Issaragrisil, S.; le Coutre, P.; Etienne, G.; Lobo, C.; Pasquini, R.; Clark, R. E.; Hochhaus, A.; Hughes, T. P.; Gallagher, N.; Hoenekopp, A.; Dong, M.; Haque, A.; Larson, R. A.; Kantarjian, H. M. *New Engl. J. Med.* **2010**, 362, 2251.
56. Parkkila, S.; Innocenti, A.; Kallio, H.; Hilvo, M.; Scozzafava, A.; Supuran, C. T. *Bioorg. Med. Chem. Lett.* **2009**, 19, 4102.
57. Shimazaki, C.; Ochiai, N.; Uchida, R.; Fuchida, S.-I.; Okano, A.; Ashihara, E.; Inaba, T.; Fujita, N.; Nakagawa, M. *Leukemia* **2003**, 17, 804.
58. Sadis, S.; Mukherjee, A.; Olson, S.; Dokmanovich, M.; Maher, R.; Cai, C.-H.; Vu, L.; Crawford, M.; Fedechko, R.; Whitfield, L.; Stock, T.; Hellio Le Graverand-Gastineau, M.-P.; Zeiher, B. *Arthritis Rheum.* **2009**, 60, 408. doi:10.1002/art.25491.
59. Roth, H.-J. *Curr. Opin. Chem. Biol.* **2005**, 9, 293.
60. Tanimoto, S.; Pavlidis, T. A. *Comput. Graph Image Process.* **1975**, 4, 104.
61. Okuda, K.; Golub, T. R.; Gilliland, D. G.; Griffin, J. D. *Oncogene* **1996**, 13, 1147.
62. Sattler, M.; Salgia, R.; Okuda, K.; Uemura, N.; Durstin, M. A.; Pisick, E.; Xu, G.; Li, J. L.; Prasad, K. V.; Griffin, J. D. *Oncogene* **1996**, 12, 839.
63. Golub, T. R.; Barker, G. F.; Lovett, M.; Gilliland, D. D. *Cell* **1994**, 77, 307.
64. Faller, B.; Grimm, H. P.; Loeuillet-Ritzler, F.; Arnold, S.; Briand, X. *J. Med. Chem.* **2005**, 48, 2571.
65. Ertl, P.; Rohde, B.; Selzer, P. *J. Med. Chem.* **2000**, 43, 3714.